PHOTOMETRIC CALIBRATION OF THE FAINT OBJECT SPECTROGRAPH AND OTHER HST SCIENTIFIC INSTRUMENTS

R. C. Bohlin and J. D. Neill
Space Telescope Science Institute

Instrument Science Report CAL/FOS-084
presented at the ST-ECF/STScI HST Workshop in Baia Chia, 1992 July

ABSTRACT

The absolute photometric calibration of the Faint Object Spectrograph (FOS) is derived from observations of three spectrophotometric standard stars (BD+28 4211, BD+75 325, and HZ-44) in the large 4.3" entrance aperture for 14 detector-disperser combinations (six for the blue digicon, eight for the red). Observations of the three stars are used from five epochs between 1991.4 and 1992.0 for each of the blue and red digicons. Absolute calibrations for four smaller single entrance apertures are computed from a set of transmission measurements relative to the 4.3" aperture at one epoch for each side. Observations that span the time interval from 1991.0 to 1992.2 show a decrease in the sensitivity for the blue digicon of about 10% per year at all wavelengths, while the red digicon has a sensitivity that is constant to 5%, except in the wavelength range of 1800-2100A, where the decrease in sensitivity is also roughly 10% per year. After correcting for these sensitivity losses and after considering the sensitivity changes caused by the OTA focus changes, the FOS spectrophotometry in the 4.3" aperture has an internal consistency of a few percent.

Preliminary GHRS flux distributions derived from observations of BD+28 4211 in the Large Science Aperture are consistent with the FOS to 5%. Since the primary WFPC flux standard is BD+75 325, the absolute calibrations of the default chips WF2 and PC6 are also on the same absolute flux scale to the accuracy that the changing sensitivity can be tracked. Longward of the F336W filter, WFPC photometry is good to 5-10%.

1. INTRODUCTION

Each spectrophotographic mode has an absolute calibration or inverse sensitivity (S^-1) that can be used to derive the flux of a point source by F = S^-1 * C, where F is the flux of the source and C is the observed counts per second. The S^-1 curve can be calculated from the count rates of stars with known fluxes.

The original S^-1 curves were derived from the laboratory calibration of the FOS and estimates of the OTA efficiency. During the early phase of orbital science verification, spanning the time from 1990.9 to 1991.0, HST observations of standard stars generated the first set of S^-1 curves that were installed in the production data processing on 1991 March 6. Since mid-1991, the focus of the observatory has stablized, and the geomagnetic image motion (GIM) problem has been addressed (Hartig et al. 1992). The current set of S^-1 curves that was installed in the production pipline on 1992 March 30 is derived from observations of three standard stars between 1991.4 and 1992.0. This 1991.4 - 1992.0 calibration differs from the 1990.9 - 1991.0 set by a maximum of 20% for the prism calibrations and will be used for the complete reprocessing of the HST data archive. The difference between the 91Mar6 and the 92Mar30 calibrations for the high dispersion FOS gratings are typically less than 10-15%.

2. STANDARD STAR SELECTION AND OBSERVATION

Five standard stars are selected from the IUE standards of Bohlin et al. (1990). The three stars BD+75 325, BD+33 2642, and BD+28 4211 have been used to monitor the changes in IUE sensitivity and have the best measured UV flux distributions. The star G191B2B (WD0501+527) is selected because of its well determined flux and a featureless continuum that is used to determine the FOS flat field correction (Keyes 1992). The star HZ-44 is selected to extend the magnitude range to 9.5 - 11.8 in the V band. The fluxes of these stars at visual wavelengths were measured by Oke (1990).

A single measurement of the FOS sensitivity is calculated from an observation of one of the program stars using a unique combination of digicon, disperser, and the 4.3" aperture. Each observation has an overscan value of 5 and an nxstep value of 4. The nxstep value of 4 defines the pixel subsampling with respect to the diode resolution elements at four pixels per diode, i.e. 12.5 micron substeps and 50 micron wide diodes. To avoid loss of light due to the GIM offset in the y direction (Hartig et al. 1992), three ysteps are centered on the nominal ybase with a spacing of 10.66 ybase units (8.33 microns).

Each observation is converted from raw counts to counts per second, de-GIMed, corrected for detector non-linearity (Lindler and Bohlin 1988), and flat fielded (Anderson 1992) to yield the observed count rate. The scattered light and residual dark count are subtracted before the flat field division for observations with the blue digicon using the G130H or G160L dispersers and with the red digicon using the G190H, G780H, G160L, G650L, or PRISM dispersers. These configurations have regions where the response to dispersed light is zero and where the background can be measured. For other configurations, the scattered light can not be measured but adds a sytematic error of less than 1% to the S^-1 curves for these configurations. To remove the small-scale effects of the pixel-to-pixel response which varies over time in the wavelength region of 1800-2100A on the red side, the flat field corrections (Keyes 1992) for the G190H, G270H, and G160L dispersers is linearly interpolated in time between bracketing flat field observations. With the exception of the scattered light subtraction and the flat field interpolation, these steps are performed using standard CALFOS routines, which duplicate the routine post observation data processing system (PODPS) reductions.

3. INVERSE SENSITIVITY CURVES

3a. DERIVATION

The S^-1 curves are calculated for the 14 most useful detector-disperser combinations of the FOS in the 4.3" aperture. S^-1 curves for the other single apertures are calculated from these curves and the throughput ratios measured by separate observations. Neill, Bohlin, and Hartig (1992) provide more details of the FOS absolute calibration process.

A single measurement of the S^-1 for a given configuration is derived from the ratio of the known flux spectrum of the source in ergs s^-1 cm^-2 A^-1 to the observed count rate spectrum. The observed count rate array is read and the three ysteps are examined. The ystep with the highest count rate is used for the calculation; and the other two ysteps are included if their countrate is within 0.5% of the highest ystep. For all dispersers except the PRISM, the observed count rate distribution is resampled to match the published flux distribution using a trapezoidal integration with limits defined as the midpoints between the wavelengths of the standard star spectrum. The non-linear dispersion of the PRISM requires that the published flux distribution be

resampled to match the count rate distribution wavelengths using the same technique. A bi-cubic spline is fit to the ratio points and the resulting spline coefficients are used to generate the S^-1 curve over the required wavelength range. Node positions for the splines depend only on the disperser with the exception of G160L, which has different node positions for the blue and red digicon. In most cases, the nodes are placed at specific wavelengths to follow features but are sometimes evenly spaced across the wavelength range.

For dispersers that include wavelengths near 3200A, a mask is employed to avoid the range 3100-3350A, the region where the IUE measurements are joined to the ground based observations. The match is not always smooth in this region due to the low sensitivity of the IUE and the difficulty in obtaining ground based absolute fluxes.

The set of S^-1 curves for the smaller single apertures is generated by applying the throughput ratio for the given aperture with respect to the 4.3" aperture. The ratios are fit with a polynomial of order 1 as a function of wavelength, except the red side G190H configuration, which is fit with a polynomial of order 2 due to stronger curvature in the aperture ratio function. See Figure 1 for an example.

3b. DATA DISTRIBUTION

The S^-1 curves are available in digital form on the STSCIC VAX cluster at the Space Telescope Science Institute (STScI). STSDAS compatable GEIS files can be found in DISK$REFERENCE:[CDBSDATA.REFER.YREF] in the files with extensions of .r2h and .r2d. If direct access to this system is not available, then contact the User Support Branch at the STScI or the European Coordinating Facility.

4. TREND ANALYSIS

Figure 2 shows the worst case of the decreasing FOS sensitivity on the red G190H grating (Hartig 1991). In order to study the change of FOS sensitivity with time, the effect of the changing focus of the telescope (OTA) on the transmission through the FOS apertures must be computed. Figure 3 is an example of this transmission change for the 4.3" acquisition aperture, which is limited to 1.4" in one dimension by the height of the FOS diodes.

Figure 4 shows examples of the trend of FOS sensitivity with time through the 4.3" aperture within broad wavelength bands with respect to the 1992 Mar 30 delivery. A correction to the observed sensitivity is included in Figure 4 for the changes of Figure 3. The blue side exhibits a steady downward trend in sensitivity of about 10% per year. The red side shows a constant sensitivity to within about 5% over the same time period with the exception of the G190H, and G160L dispersers, which exhibit a downward trend in the 1800 to 2100A range. Since the most recent data from mid-1992 shows large deviations from the solid lines, more data is required to predict the FOS sensitivity to better than 5% with a high confidence level.

6. FUTURE WORK

A set of S^-1 curves with better accuracy will be derived by accounting for the sensitivity changes over time. The S^-1 curves for the paired apertures will also be calculated.

A collateral benefit of the FOS calibration program will be an improved network of flux distributions for standard stars from 1150 to 8500A. Without the complications of an intervening atmosphere, more accurate relative spectrophotometry should be possible with FOS than has been achieved before over such a large wavelength range. The current data shown in Figure 4 already demonstrate a problem with the reference spectrophotometry for BD+33 2642. Comparisons of the Oke (1990) fluxes to FOS fluxes for BD+33 2642 show a systematic offset. Therefore, observations of BD+33 2642 are not included in the 1991.4-1992.0 average calibrations. This offset for BD+33 2642 in the published flux values can also be seen in the trend analysis (see next section and Figure 4). An ultimate relative accuracy on the order of 1% should be achievable, as suggested by Figure 5.

7. OTHER INSTRUMENTS

The other spectrophotometer on HST with appropriate spectral dispersion is the GHRS low dispersion grating on the currently disabled Side 1. However, accurate relative fluxes can be derived from medium resolution GHRS observations, as shown in Figure 6.

The WFPC photometry is on the same basis as the spectrometers, since the primary standard is BD+75 325. Longward of the F336W filter, the photometric repeatability is 5-10% (Sparks, Richie, and MacKenty 1992). For the shorter wavelength filters, the contamination changes too rapidly to track the absolute sensitivity well (Richie and MacKenty 1992).

Unfortunately, the FOC cannot observe such bright stars photometrically; and the FOC slit is too narrow to achieve good spectrophotometry of point sources.

8. REFERENCES

Anderson, S. F. 1992, FOS Instrument Science Report 075.

Bohlin, R. C., Harris, A. W., Holm, A. V., Gry, C. 1990, Ap. J. Suppl., 73, 413.

Hartig, G. 1991, FOS Instrument Science Report 69.

Hartig., G., Lindler, D., Beaver, E., Junkkarinen, V., and Lyons, R. 1992, FOS Instrument Science Report, in preparation.

Keyes, A. 1992, private communication.

Lindler, D., and Bohlin, R. 1988, FOS Instrument Science Report 45.

Neill, J. D., Bohlin, R., and Hartig G. 1992, FOS Instrument Science Report 77.

Oke, J. B. 1990, Astron. J., 99, 1621.

Richie, C. E., and MacKenty, J. W. 1992, WFPC Instrument Science Report 92-07.

Sparks, W. B., Richie, C., and MacKenty, J. 1992, WFPC Instrument Science Report 92-09.

FIGURE 1-The fractional transmission with respect to the 4.3" aperture for the circular single apertures on the red side H19 (G190H) grating. This configuration is fit with a polynomial of order 2 but has a maximum deviation of only 2% with respect to the average transmission. The aperture diameters are 1" (B-3), 0.5" (B-1), and 0.3" (B-2).

FIGURE 2-The red-side G190H sensitivity degradation, which has a high frequency fixed pattern and a 200A broad continuum trough. (See Figure 4c for the rate of loss in the trough center at 1950A.) Starting in 1991 December, monthly monitoring of the changing fine structure provides corrections for FOS flat fields to about 2% accuracy for the effected red side observations. Laboratory irradiation of a spare fused silica faceplate for the red side Digicon with the equivalent of 3 years of on-orbit radiation failed to produce any similar transmission loss, nor is there any such degradation on the FOS blue side.

FIGURE 3-The relative flux for a point source that is transmitted by a 1.4x4.3 arcsec FOS aperture, computed per the presciption of C. Burrows, STScI Instr. Sci. Report OTA 7, 1992 Feb. The discontinuities are at the times of major adjustments of the HST secondary mirror, while the smooth changes in transmission are due to the desorption of water in the graphite epoxy metering truss.

FIGURE 4- The sensitivity change with respect to the baseline 1992 March 30 absolute calibration for the 4.3" aperture in selected wavelength bands for four grating/detector combinations. The heavy solid line is a linear fit to the points that are connected by the thin lines. Corrections for changes in the HST focus have been applied per Figure 3 to isolate the true change of the FOS sensitivity. The 5 sets of observations between 1991.4 and 1992.0 define the 1992 March 30 baseline. BD+33 2642 is excluded from consideration, because the visible calibration is not consistent with the other four stars.

FIGURE 5-FOS fluxes for BD+75 325 after applying both the mean red side calibrations and the correction for the changing red-side G190H sensitivity. Three sets of observations of BD+75 325 for five high dispersion gratings are co-added and merged. The standard star flux distribution is increased by a factor of 1.2 for display; and both spectra are multiplied by the function (wavelength/10000)^3.5 to permit an expanded scale on the ordinate. The ratios of the FOS fluxes to the standard star fluxes demonstrate an internal consistency of better than 2%.

FIGURE 6-Comparison of GHRS measured fluxes with the standard star BD+28 4211. The triangles at the bottom are the ratios of GHRS absolute fluxes to the standard star in 3 wavelength bins for each of 5 medium-resolution grating positions on side 2. The GHRS fluxes agree with the standard to a few percent and demonstrate a sensitivity that is constant to a couple percent over the 115 day interval. The absolute calibration is based on mu Col (Final SV Report for the GHRS 1992 Feb.)

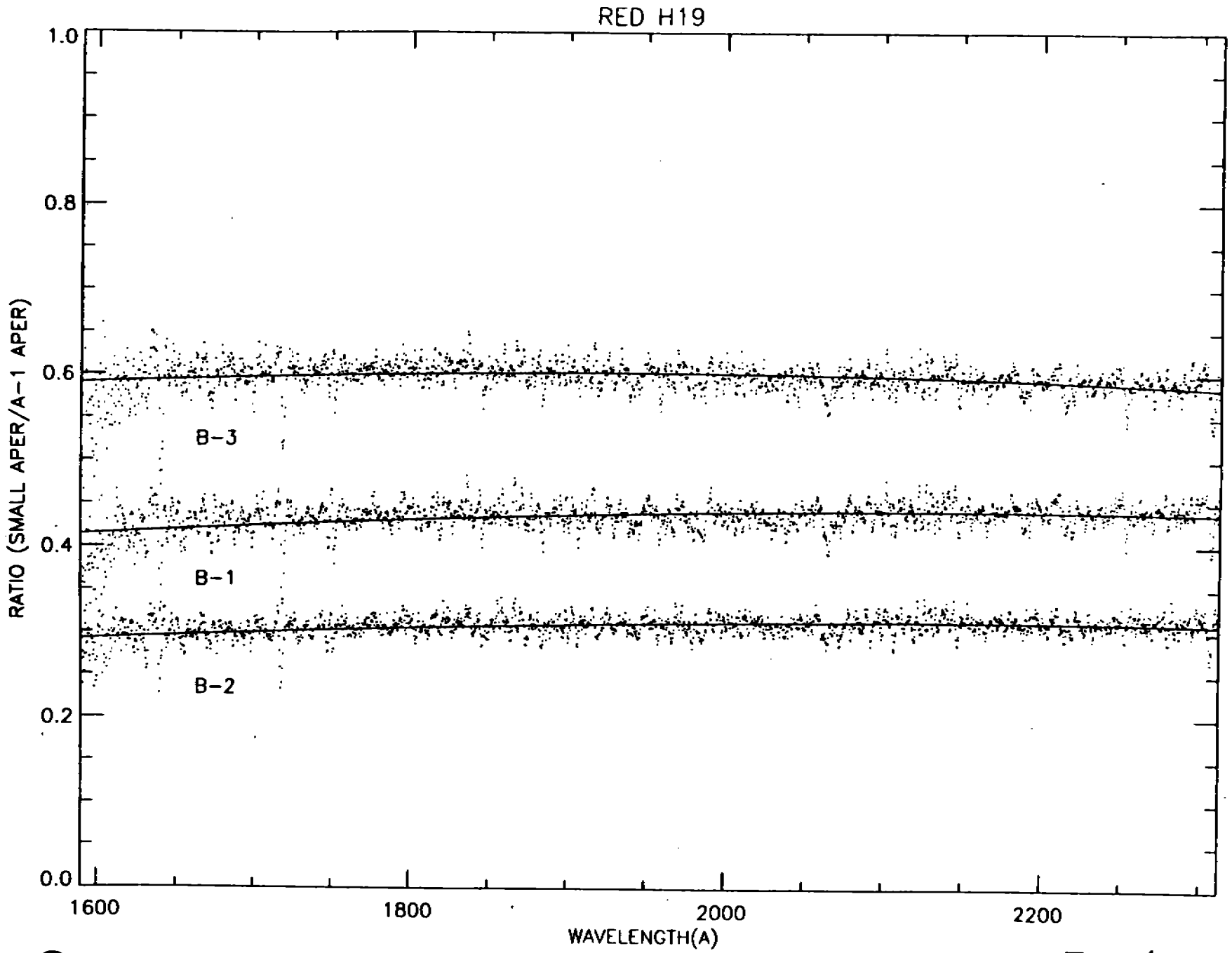
RED H19
1.0
0.8
0.6
0.4
0.2
0.0
RATIO (SMALL APER/A-1 APER)
B-3
B-1
B-2
1600
1800
2000
2200
WAVELENGTH(A)

Fig. 1

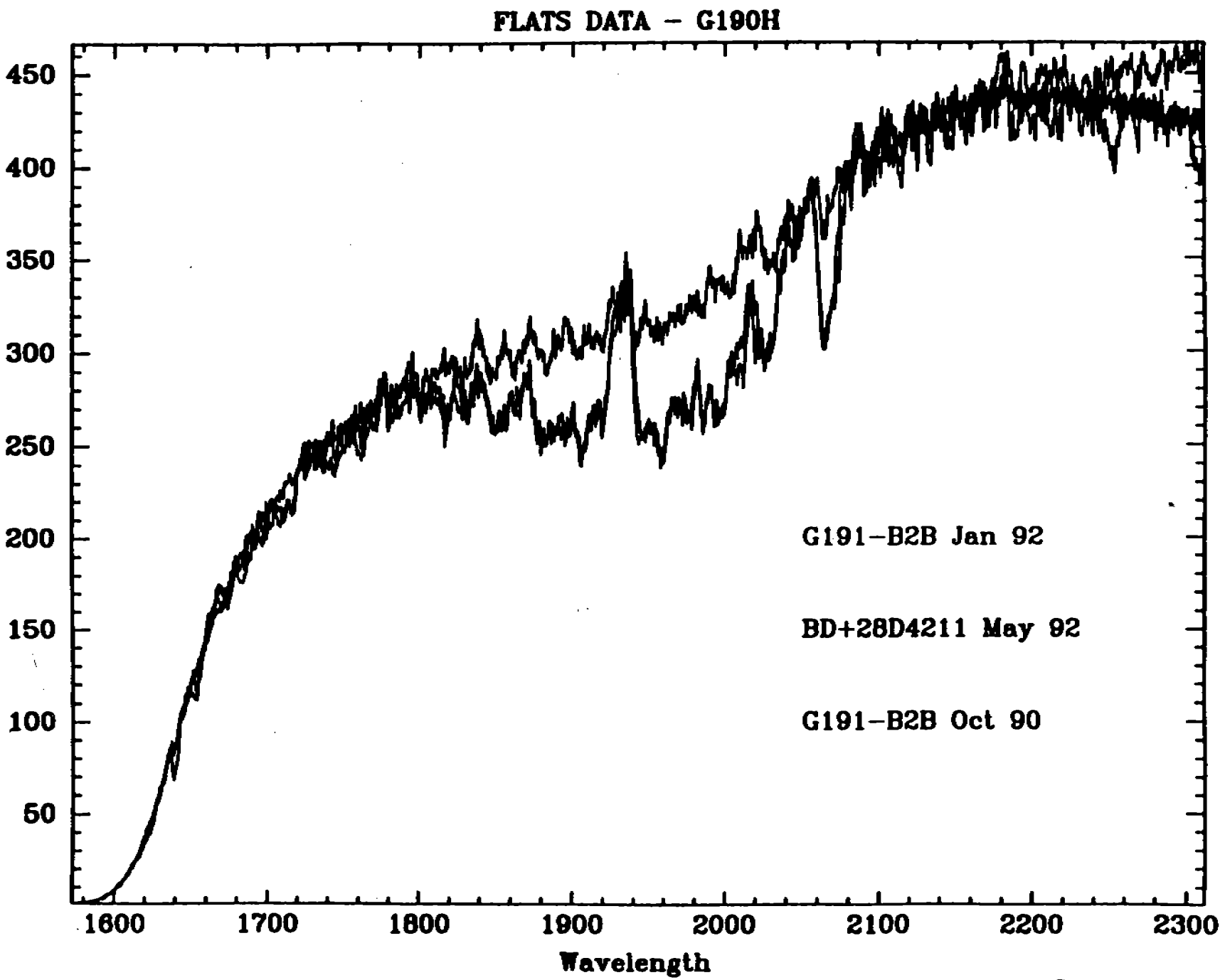
FLATS DATA – G190H
450
400
350
300
250
200
150
100
50
1600
1700
1800
1900
2000
2100
2200
2300
Wavelength
G191–B2B Jan 92
BD+28D4211 May 92
G191–B2B Oct 90

Fig. 2

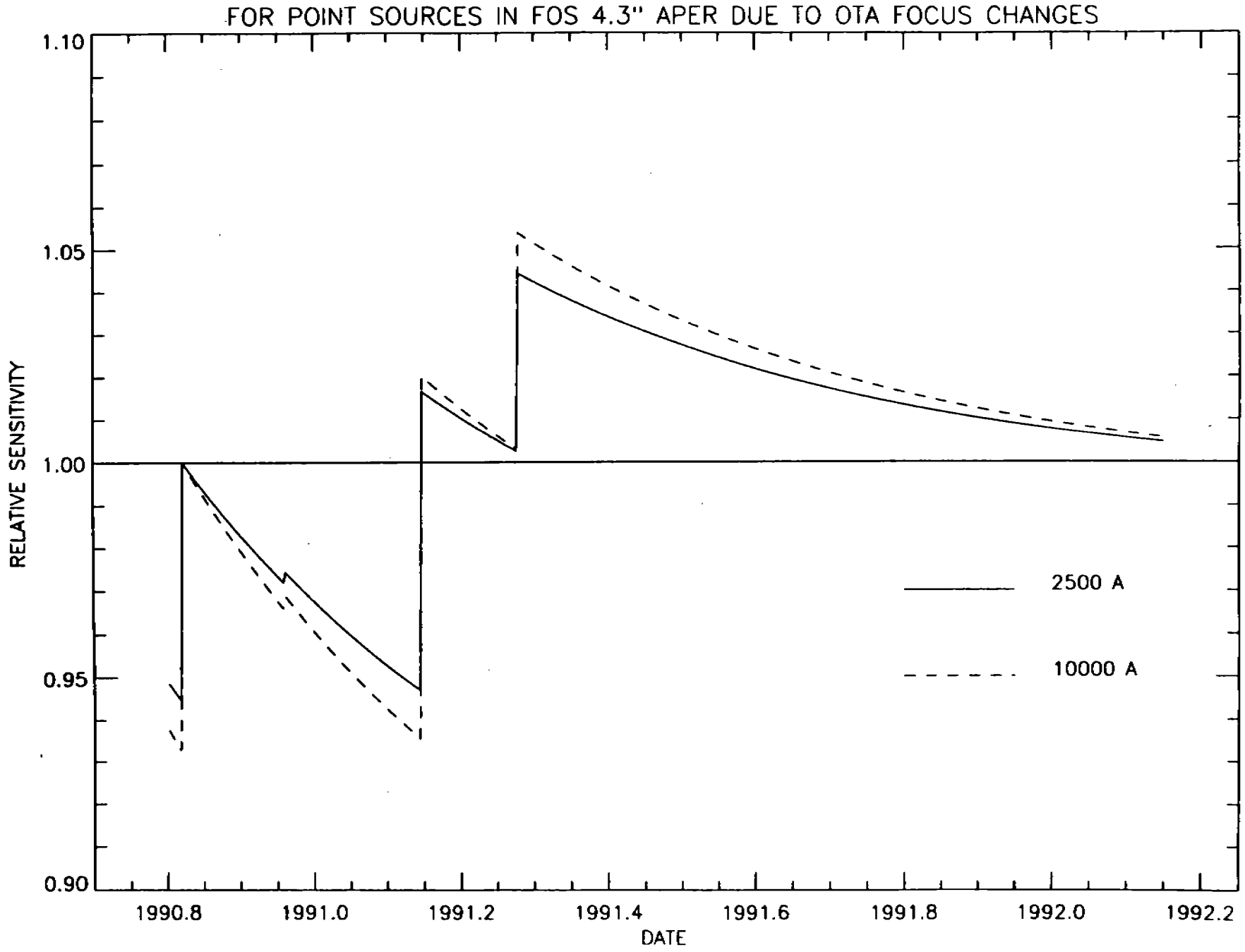
FOR POINT SOURCES IN FOS 4.3" APER DUE TO OTA FOCUS CHANGES
RELATIVE SENSITIVITY
1.10
1.05
1.00
0.95
0.90
1990.8
1991.0
1991.2
1991.4
1991.6
1991.8
1992.0
1992.2
DATE
2500 A
10000 A

Fig. 3

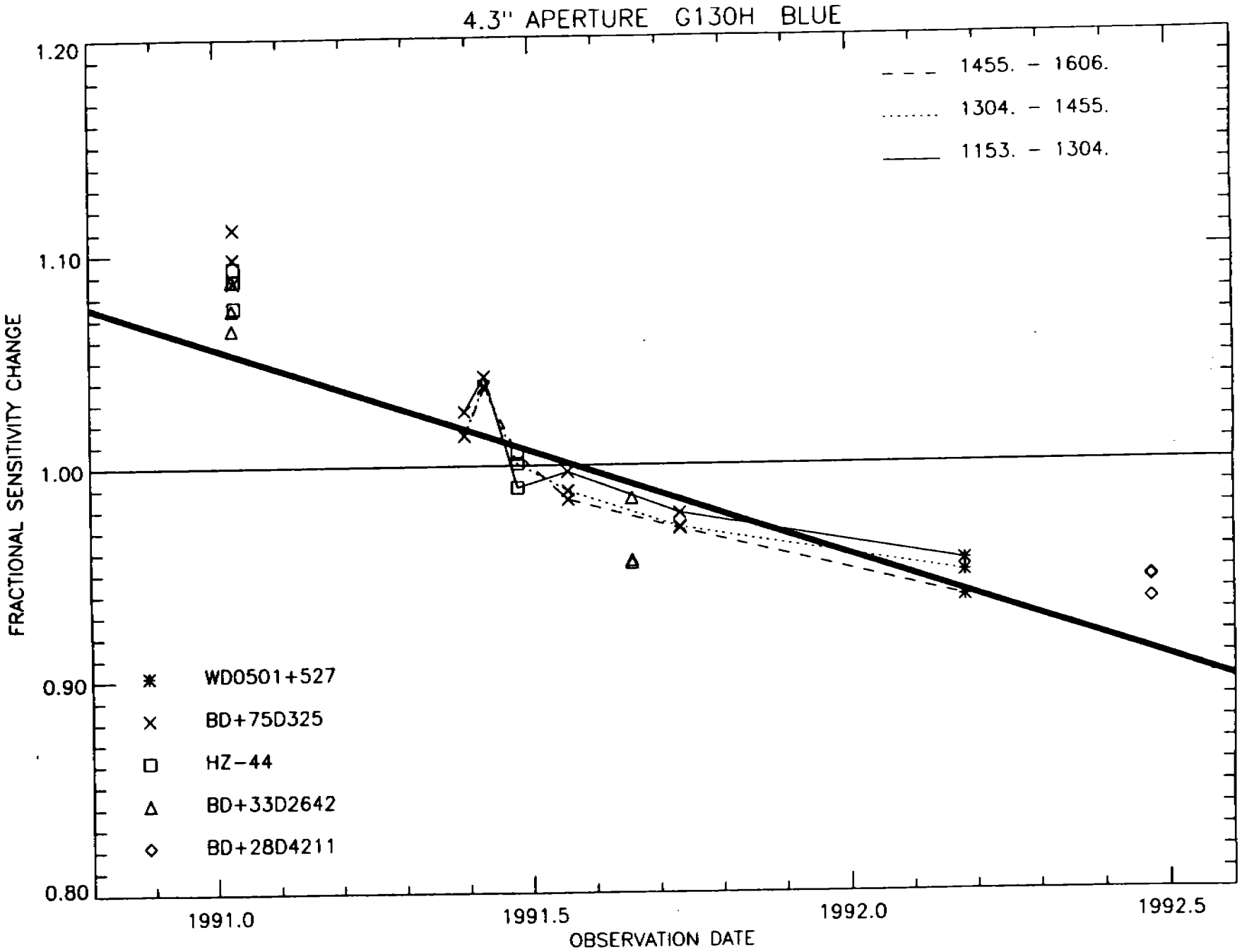
4.3" APERTURE G130H BLUE
1455. - 1606.
1304. - 1455.
1153. - 1304.
FRACTIONAL SENSITIVITY CHANGE
1.20
1.10
1.00
0.90
0.80
WD0501+527
BD+75D325
HZ-44
BD+33D2642
BD+28D4211
1991.0
1991.5
1992.0
1992.5
OBSERVATION DATE

Fig. 4a

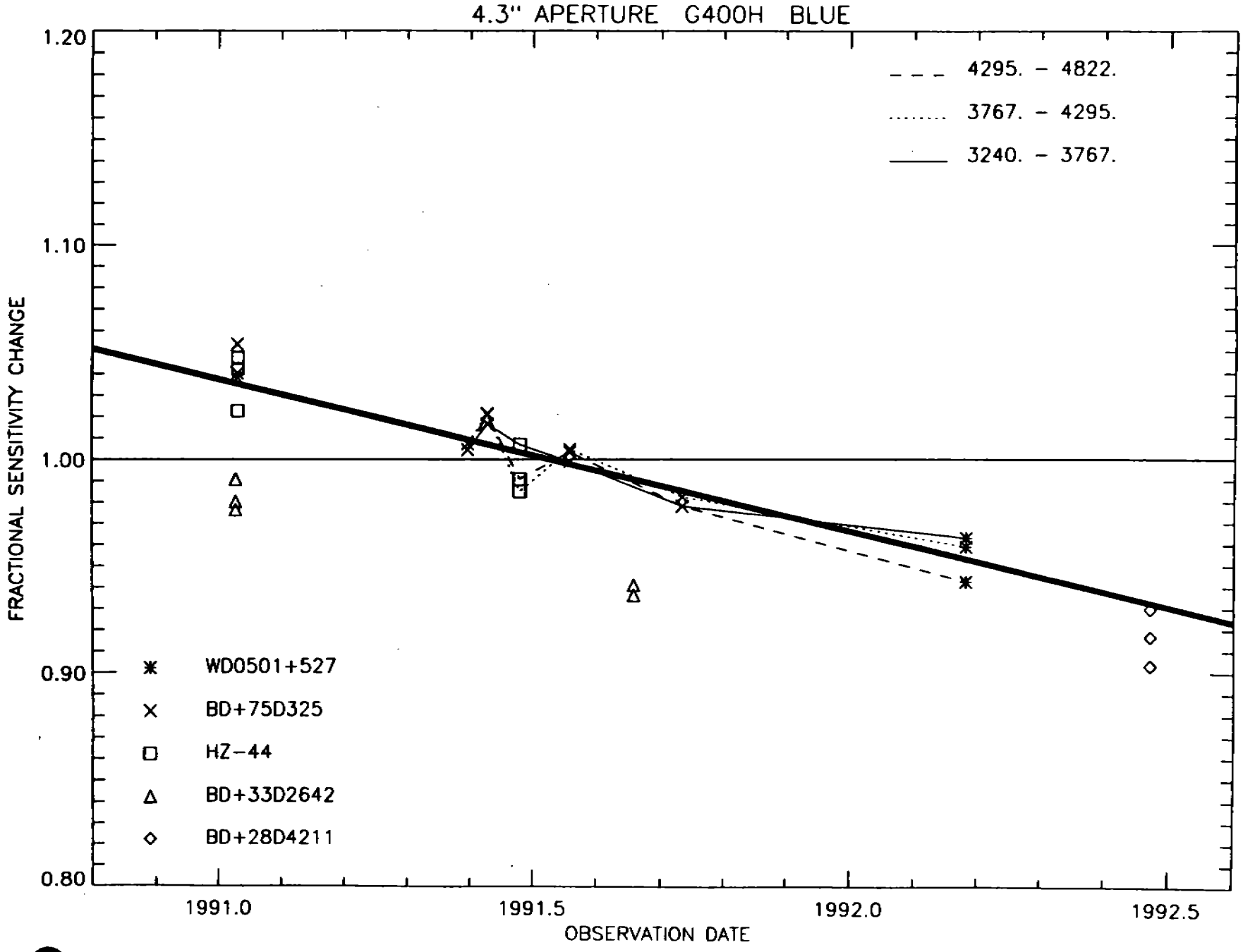
4.3" APERTURE G400H BLUE
4295. - 4822.
3767. - 4295.
3240. - 3767.
FRACTIONAL SENSITIVITY CHANGE
1.20
1.10
1.00
0.90
0.80
WD0501+527
BD+75D325
HZ-44
BD+33D2642
BD+28D4211
1991.0
1991.5
1992.0
1992.5
OBSERVATION DATE

Fig. 4b

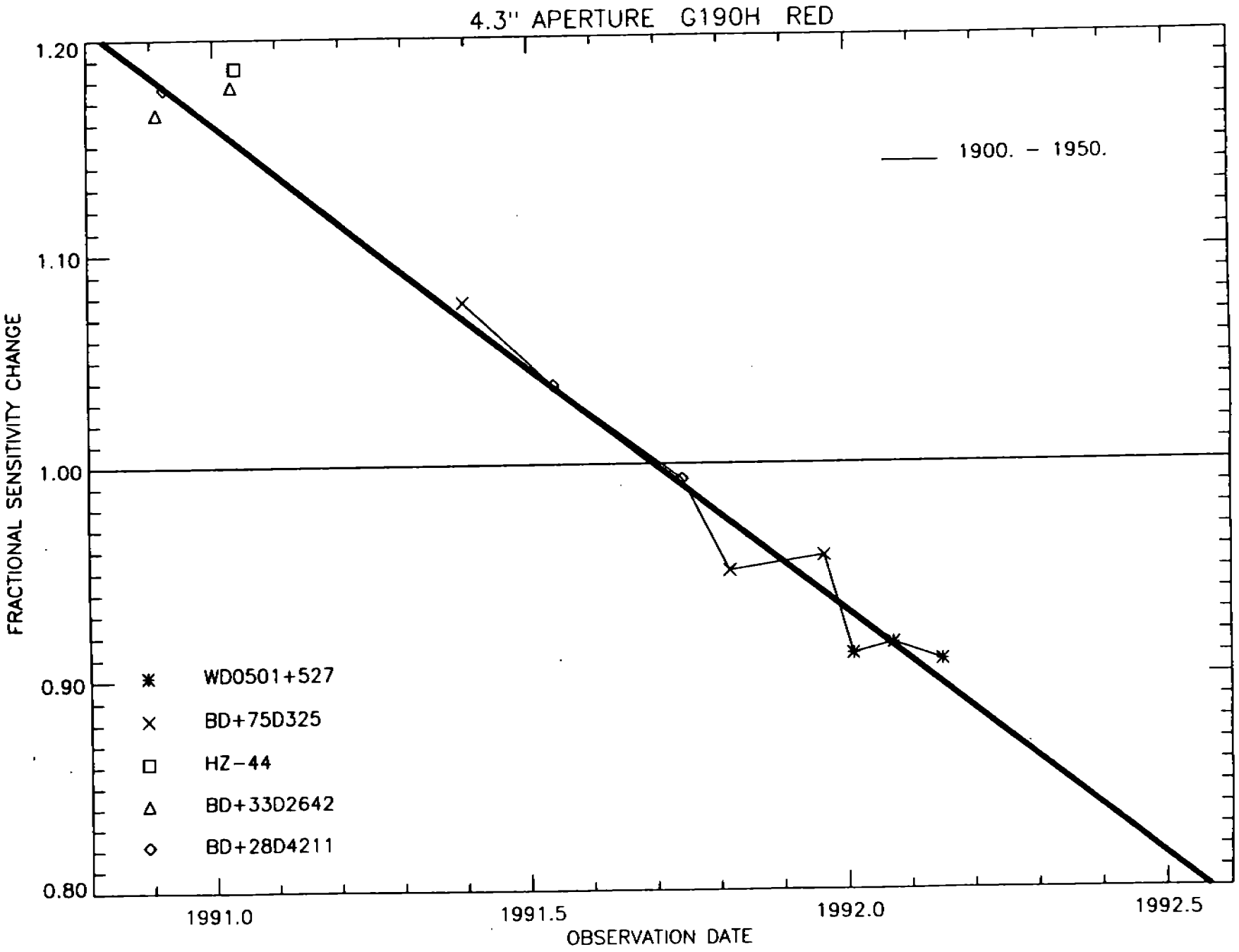
4.3" APERTURE G190H RED
1.20
1.10
1.00
0.90
0.80
FRACTIONAL SENSITIVITY CHANGE
1900. – 1950.
WD0501+527
BD+75D325
HZ-44
BD+33D2642
BD+28D4211
1991.0
1991.5
1992.0
1992.5
OBSERVATION DATE

Fig. 4c

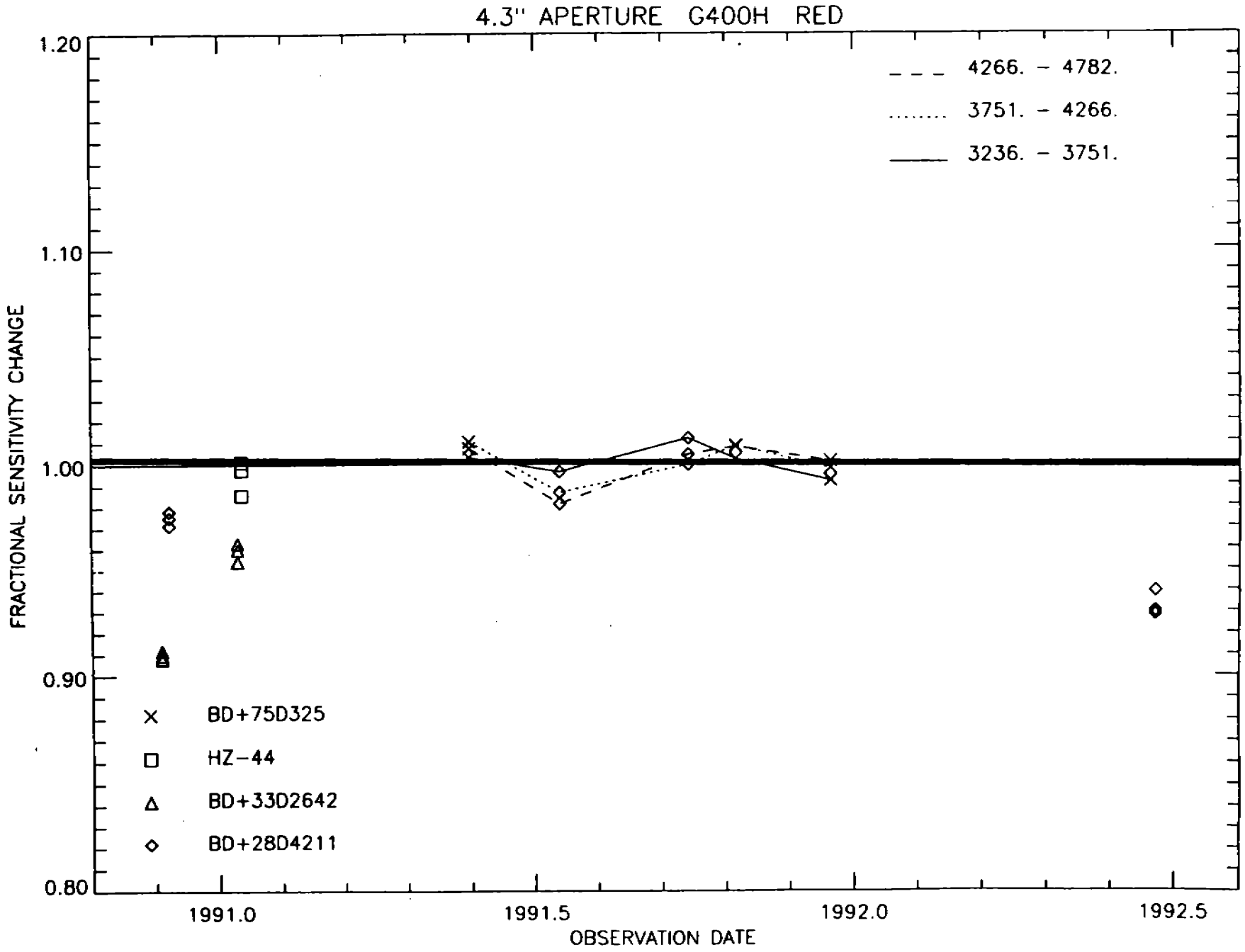
4.3" APERTURE G400H RED
4266. - 4782.
3751. - 4266.
3236. - 3751.
FRACTIONAL SENSITIVITY CHANGE
1.20
1.10
1.00
0.90
0.80
BD+75D325
HZ-44
BD+33D2642
BD+28D4211
1991.0
1991.5
1992.0
1992.5
OBSERVATION DATE

Fig. 4d

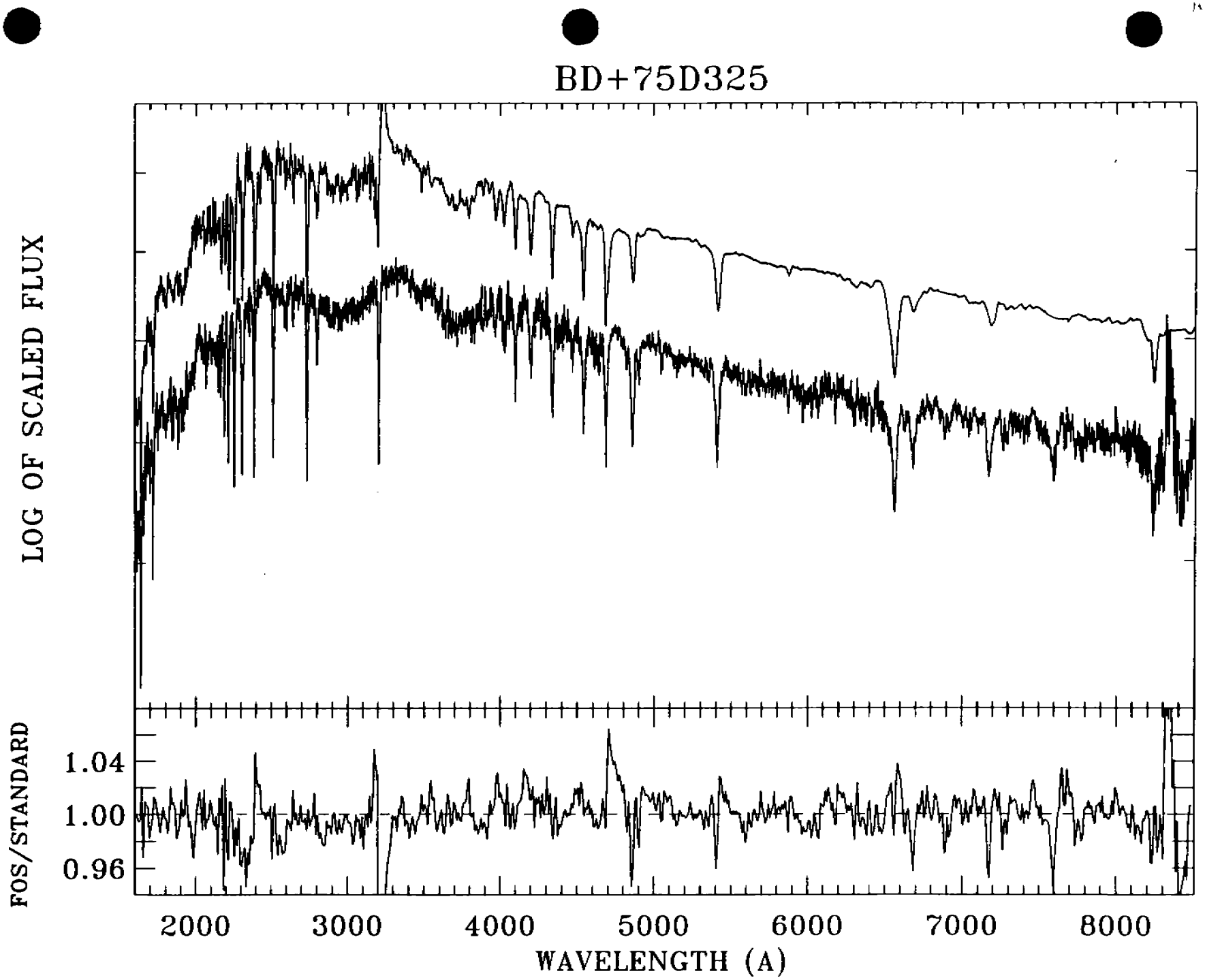
BD+75D325
LOG OF SCALED FLUX
FOS/STANDARD
1.04
1.00
0.96
2000
3000
4000
5000
6000
7000
8000
WAVELENGTH (A)

Fig. 5

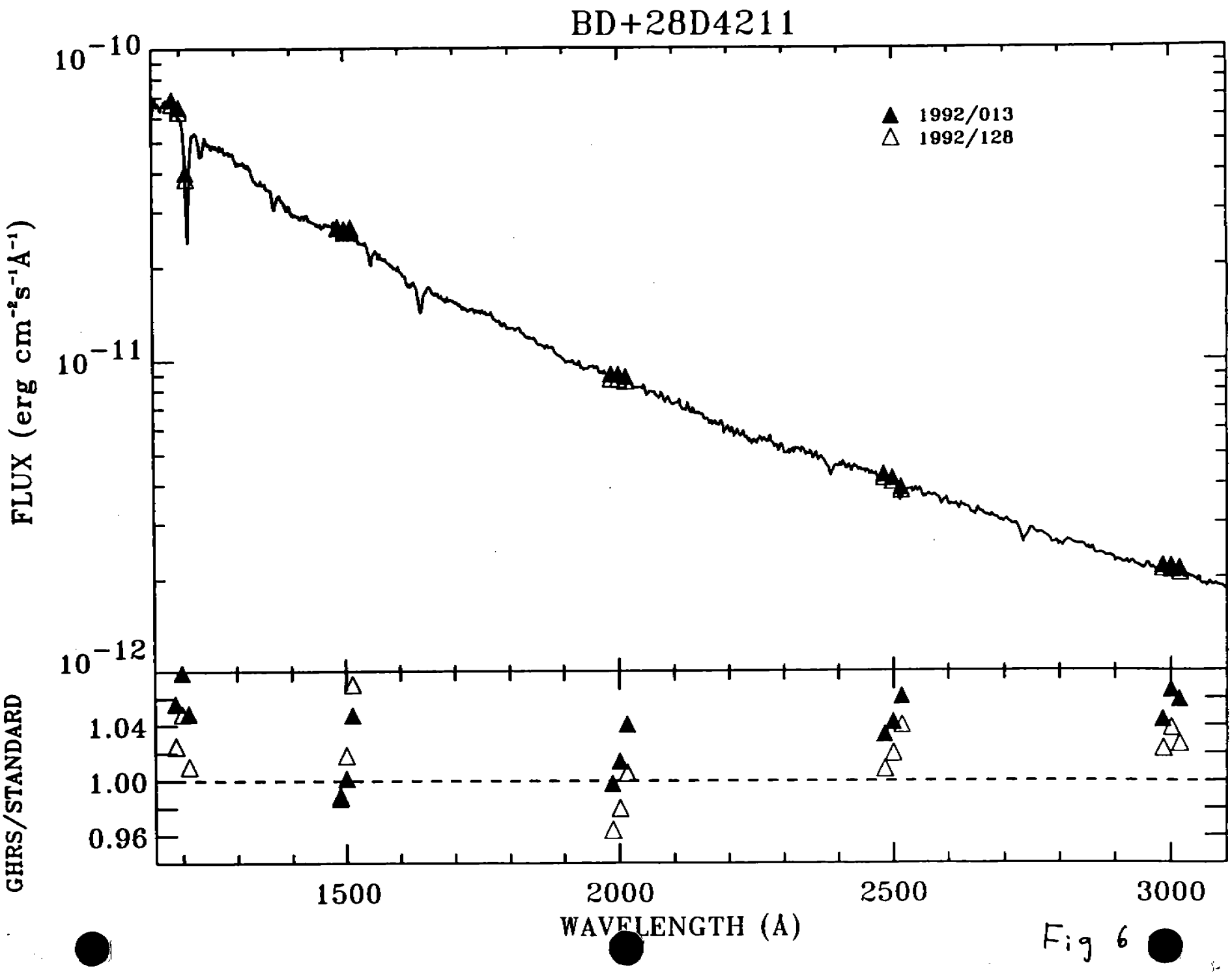
BD+28D4211
1992/013
1992/128
FLUX (erg cm⁻²s⁻¹A⁻¹)
10⁻¹⁰
10⁻¹¹
10⁻¹²
GHRS/STANDARD
1.04
1.00
0.96
1500
2000
2500
3000
WAVELENGTH (A)

Fig 6